

## Role of the C-10 Substituent in Mitomycin C-1–DNA Bonding

Ven-Shun Li,<sup>†</sup> Daeock Choi,<sup>†</sup> Zheng Wang,<sup>‡</sup> Leslie S. Jimenez,<sup>‡</sup> Moon-shong Tang,<sup>\*,§</sup> and Harold Kohn<sup>\*,†</sup>

Contribution from the Department of Chemistry, University of Houston, Houston, Texas 77204-5641, Department of Chemistry, Rutgers University, Piscataway, New Jersey 08855-0939, and Science Park-Research Division, M. D. Anderson Cancer Center, The University of Texas System, Smithville, Texas 78957

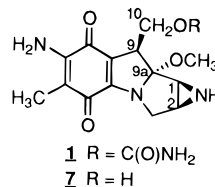
Received November 17, 1995<sup>⊗</sup>

**Abstract:** The structural requirements for mitomycin C-1 bonding have been investigated by comparing the bonding specificity of mitomycin C (**1**) with selectively modified porfiromycins (*N*-methylmitomycin C) at the C-10 position under reductive conditions and then comparing *N*-methyl-7-methoxyaziridinomitosene (**10**) with 7-methoxy-10-noraziridinomitosene (**11**) under nonreductive conditions. Enzymatic and chemical reductive activation of mitomycin C in the presence of the 129-bp fragment from pBR322 led to exclusive guanine (G\*) modification with drug bonding that occurred preferentially at 5'CG\* sites, while C-10 chloro (**8**) and C-10 bromo (**9**) deoxycarbamoylporfiromycins modified DNA at guanines but with significantly diminished 5'CG\* sequence selectivity. A similar set of bonding profiles were observed with **10** and **11** upon incubation with DNA. Mitosene **10** selectively modified 5'CG\* sites in DNA, while **11** did not. These studies provided support for the hypothesis that a hydrogen bond between the C-10 oxygen in the activated mitomycin species and the guanine N(2)-amino proton on the nonbonding DNA strand in the precovalent complex permits selective modification of 5'CG\* sites in *in vitro* transformations. We have also found that the kinetics of UVRABC incision of *N*-methyl-7-methoxyaziridinomitosene (**10**)–DNA adducts at different sequences are identical. This finding leads us to conclude that drug modification-induced UVRABC incision at different sites represents the sequence selectivity of drug–DNA bonding.

Extensive screening programs have led to the discovery of natural products that exhibit selective bonding to DNA and possess potent antitumor antibiotic activities. Most of these compounds contain an extensive array of structural and topological features that permit the drug to dock at specific sites in the DNA, allowing for a latent reactive site in the drug to cause a lesion in DNA. This event is believed to be the primary source of the anticancer activity.<sup>1</sup> In many of these compounds, the observed site and DNA sequence selectivity emanates from the conformational, electrostatic, hydrogen bonding, dipole–dipole, and van der Waal interactions that take place between the drug and the DNA surface during the initial drug binding event.<sup>1</sup>

Mitomycin C (**1**), unlike many naturally occurring anticancer drugs, is a small, compact compound.<sup>2</sup> Despite what seems to be a structural deficit, **1** preferentially bonds to select DNA sequences (Scheme 1).<sup>3</sup> It has been demonstrated that *in vitro* mitomycin C monoalkylation transformations that provide **5** proceed only at guanine (G\*) sites, with 5'CG\* dinucleotide sequences being modified at appreciably higher levels than 5'AG\*, 5'GG\*, and 5'TG\* sequences,<sup>4–6</sup> and that *in vitro* and *in vivo* mitomycin C–DNA bisalkylation, interstrand cross-

linking processes to give **6** occur within complementary 5'CG\* sequences rather than at 5'G\*C sequences.<sup>7–9</sup>



The parameters that govern the drug–receptor site interactions leading to the initial DNA alkylated product **5** have not been fully elucidated. The Remers,<sup>10</sup> Tomasz,<sup>5</sup> and Kohn<sup>6</sup> groups have suggested that mitomycin C monoalkylation reactions that proceed at 5'CG\*·5'CG sequences are facilitated, in part, by the formation of a hydrogen bond between the C-10 oxygen of the activated mitomycin species and the N(2)-amino proton on the guanine (G) of the nonbonding strand (Figure 1). This arrangement is expected to promote monoalkylation of DNA by **1** by positioning the activated drug near a guanine (G\*) present on the bonding strand. Early support for this contention came from two sources. First, near equivalent bonding patterns

(4) Li, V.-S.; Kohn, H. *J. Am. Chem. Soc.* **1991**, *113*, 275–283.

(5) Kumar, S.; Lipman, R.; Tomasz, M. *Biochemistry* **1992**, *31*, 1399–1407.

(6) Kohn, H.; Li, V.-S.; Tang, M.-S. *J. Am. Chem. Soc.* **1992**, *114*, 5501–5509.

(7) Teng, S. P.; Woodson, S. A.; Crothers, D. M. *Biochemistry* **1989**, *28*, 3901–3907.

(8) (a) Weidner, M. F.; Millard, J. T.; Hopkins, P. B. *J. Am. Chem. Soc.* **1989**, *111*, 9270–9272. (b) Millard, J. T.; Weidner, M. F.; Raucher, S.; Hopkins, P. B. *J. Am. Chem. Soc.* **1990**, *112*, 3637–3641. (c) Weidner, M. F.; Signurdsson, S. T.; Hopkins, P. B. *Biochemistry* **1990**, *29*, 9225–9233.

(9) (a) Borowy-Borowski, H.; Lipman, R.; Tomasz, M. *Biochemistry* **1990**, *29*, 2999–3006. (b) Tomasz, M.; Lipman, R.; Chowdary, D.; Pawlak, J.; Verdine, G. L.; Nakanishi, K. *Science* **1987**, *235*, 1204–1208.

(10) Remers, W. A.; Rao, S. N.; Wunz, T. P.; Kollman, P. A. *J. Med. Chem.* **1988**, *31*, 1612–1620.

<sup>†</sup> University of Houston.

<sup>‡</sup> Rutgers University.

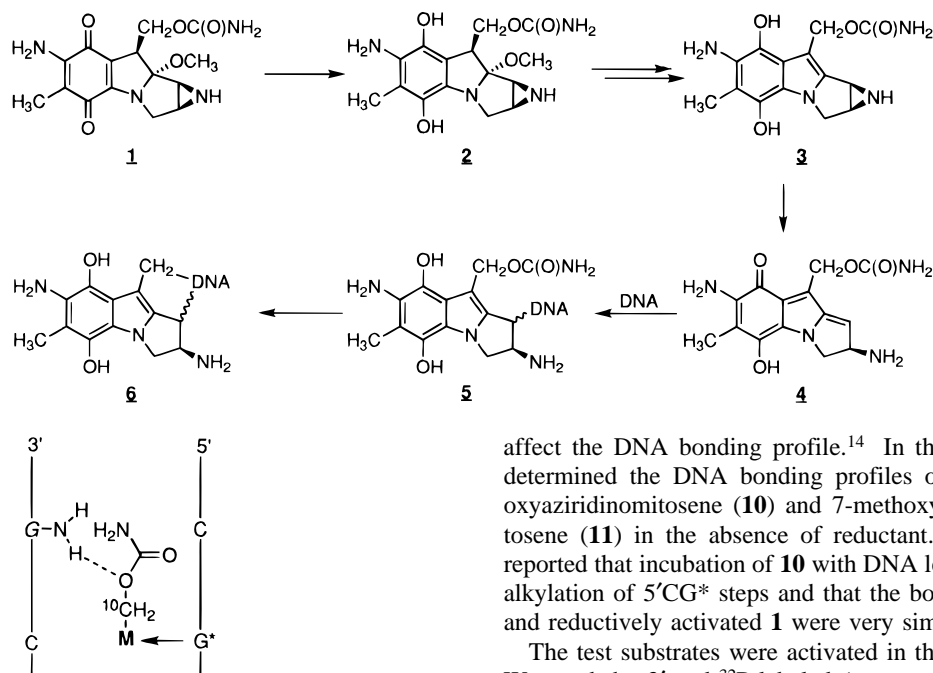
<sup>§</sup> The University of Texas System.

<sup>⊗</sup> Abstract published in *Advance ACS Abstracts*, February 15, 1996.

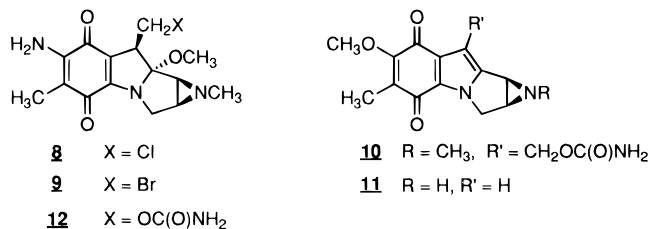
(1) (a) Warpehoski, M. A.; Hurley, L. H. *Chem. Res. Toxicol.* **1988**, *1*, 315–333. (b) Searle, M. *Prog. Nucl. Magn. Reson. Spectrosc.* **1993**, *25*, 403–480.

(2) Carter, S. K.; Crooke, S. T. *Mitomycin C. Current Status and New Developments*; Academic Press: New York, 1979.

(3) For leading reviews see: (a) Iyer, V. N.; Szybalski, W. *Science* **1964**, *145*, 55–58. (b) Moore, H. W.; Czerniak, R. *Med. Res. Rev.* **1981**, *1*, 249–280. (c) Remers, W. A. *The Chemistry of Antitumor Antibiotics*; Wiley: New York, 1979; Vol. 1, pp 221–276. (d) Franck, R. W.; Tomasz, M. In *The Chemistry of Antitumor Agents*; Wilman, D. E. V., Ed.; Blackie and Sons, Ltd.: Glasgow, Scotland, 1990; pp 379–394. (e) Fisher, J. R.; Aristoff, P. A. *Prog. Drug Res.* **1988**, *32*, 411–498. (f) Tomasz, M. In *Molecular Aspects of Anticancer Drug–DNA Interactions*; Neidle, S.; Waring, M., Eds; Macmillan: Boca Raton, FL, 1994; Vol. 2, pp 312–348.

**Scheme 1.** Proposed Mechanism for the Mode of Action of Mitomycin C**Figure 1.** Proposed alignment of the activated mitomycin C at 5'CG\*·5'CG sequences within the minor groove leading to G\* modification.<sup>5,6,10</sup> The dotted line indicates the proposed hydrogen bond.

were detected for **1** and 10-decarbomylmitomycin C (**7**), demonstrating that the carbamoyl group itself did not influence the site of drug-DNA bonding.<sup>4</sup> Then, reduced bonding specificity was observed for G\* within 5'CG\*·5'CI steps where the 2'-deoxyguanosine (G) group on the nonbonding strand had been replaced by 2'-deoxyinosine (I).<sup>5</sup> We report herein on select structural modifications of the C-10 substituent in mitomycins and mitosenes that we made in order to document this critical hydrogen bond interaction. We compare the DNA bonding profiles of mitomycin C (**1**) with the C-10 halogen porfiromycins **8** and **9**<sup>11</sup> and *N*-methyl-7-methoxyaziridinomitosenes (**10**)<sup>12</sup> with the novel 7-methoxy-10-noraziridinomitosenes (**11**).<sup>13</sup> These studies demonstrated that the C-10 oxygen substituent in activated mitomycin C plays a pivotal role in aligning the drug within the DNA minor groove, permitting C-1 bonding to occur preferentially at 5'CG\* sites.



## Results and Discussion

**A. The Experimental Design.** We studied two series of compounds. In the first series, we compared the bonding patterns of the C-10 halogen porfiromycins **8** and **9** with mitomycin C (**1**) under reductive conditions. We chose to use **1** because of its availability rather than porfiromycin (**12**), since an earlier study showed that the *N*-methyl group in **12** did not

affect the DNA bonding profile.<sup>14</sup> In the second series, we determined the DNA bonding profiles of *N*-methyl-7-methoxyaziridinomitosenes (**10**) and 7-methoxy-10-noraziridinomitosenes (**11**) in the absence of reductant. We have recently reported that incubation of **10** with DNA led to the preferential alkylation of 5'CG\* steps and that the bonding profiles of **10** and reductively activated **1** were very similar.<sup>15</sup>

The test substrates were activated in the presence of DNA. We used the 3'-end-<sup>32</sup>P-labeled (upper strand) *Bst*NI-*Eco*RI 129-bp DNA fragment from pBR322 plasmid.<sup>4,6,14,16</sup> This DNA contains 15 guanine units within the central 69-bp portion of the duplex on the top labeled strand. Embedded in this DNA region are the highest (5'CG\*G), strong (5'CG\*T, 5'CG\*C, 5'TG\*T), weak (5'AG\*G, 5'TG\*C, 5GG\*C), and very weak (5'AG\*T, 5'TG\*A) affinity mitomycin C trinucleotide bonding sites.<sup>6</sup> The sequence specificity and the degree of drug-DNA bonding were determined by UVRABC nuclease incision analysis.<sup>17,18</sup> We previously demonstrated that UVRABC nuclease specifically incises 6-7 bases 5' and 3-4 bases 3' to guanine sites modified by mitomycin C and its derivatives and that the extent of this enzyme incision is proportional to the drug concentration used for DNA modification.<sup>6,14,16</sup> Additional information follows that shows the different mitomycin-guanine lesions within the 129-bp fragment are incised by UVRABC at comparable rate constants. Therefore, we have concluded that the relative intensities of the observed incision bands generated from the UVRABC treated mitomycin-DNA adducts represented the relative degree of drug modification at each particular guanine residue in the radioactively labeled DNA fragment.

Mitomycin C (**1**) and the C-10 halogen porfiromycins **8** and **9** were activated both enzymatically (xanthine oxidase/NADH)<sup>6,14,16,19</sup> and chemically (Na<sub>2</sub>S<sub>2</sub>O<sub>4</sub>).<sup>4,6,20,21</sup> The xanthine oxidase/NADH reactions were run at 37 °C for 30 min, while the amount of Na<sub>2</sub>S<sub>2</sub>O<sub>4</sub> (0.6-1.0 equiv, three incremental additions) was tailored to the substrate. The specific Na<sub>2</sub>S<sub>2</sub>O<sub>4</sub> conditions chosen were generally based on the observation of partial consumption (20-50%) of the starting mitomycin for

(14) Kohn, H.; Li, V.-S.; Schiltz, P.; Tang, M.-s. *J. Am. Chem. Soc.* **1992**, *114*, 9218-9220.

(15) Li, V.-S.; Choi, D.; Tang, M.-s.; Kohn, H. *J. Am. Chem. Soc.*, submitted for publication.

(16) Li, V.-S.; Choi, D.; Tang, M.-s.; Kohn, H. *Biochemistry* **1995**, *34*, 7120-7126.

(17) Friedberg, E. C.; Walker, G. C.; Siede, W. *DNA Repair and Mutagenesis*; ASM Press: Washington, DC, 1995.

(18) Sancar, A.; Tang, M.-s. *Photochem. Photobiol.* **1993**, *57*, 905-921.

(19) (a) Phillips, D. R.; White, R. J.; Cullinane, C. *FEBS* **1989**, *246*, 233-240. (b) McGuinness, B. F.; Lipman, R.; Goldstein, J.; Nakanishi, K.; Tomasz, M. *Biochemistry* **1991**, *30*, 6444-6453.

(20) Tomasz, M.; Mercado, C. M.; Olson, J.; Chatterjee, N. *Biochemistry* **1974**, *13*, 4878-4887.

(21) (a) Schiltz, P.; Kohn, H. *J. Am. Chem. Soc.* **1993**, *115*, 10497-10509. (b) Schiltz, P.; Kohn, H. *Tetrahedron Lett.* **1992**, *33*, 4709-4712.

(11) Choi, D.; Yoo, B.; Colson, K. L.; Martin, G. E.; Kohn, H. *J. Org. Chem.* **1995**, *60*, 3391-3396.

(12) Danishefsky, S. J.; Egbertson, M. *J. Am. Chem. Soc.* **1986**, *108*, 4648-4650.

(13) Wang, Z.; Jimenez, L. S. *J. Org. Chem.* **1996**, *61*, 816-818.

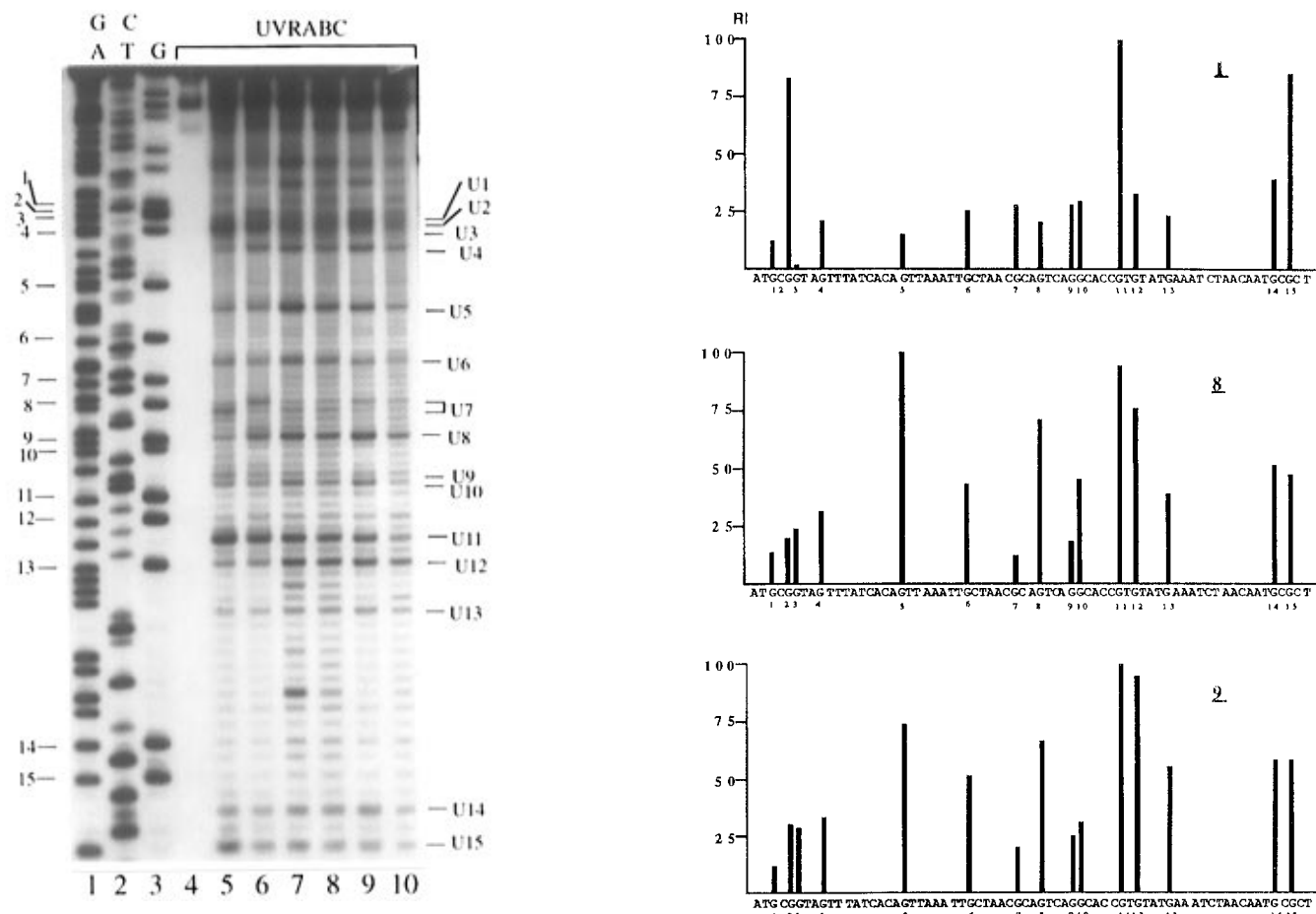


**Figure 2.** (A, left) Autoradiogram of UVRABC nuclease cutting of a mitomycin C (**1**)-modified, 10-(deoxycarbamoyl)-10-(chloro)porfiromycin (**8**)-modified, and 10-(deoxycarbamoyl)-10-(bromo)porfiromycin (**9**)-modified 3'-end- $^{32}\text{P}$ -labeled *Bst*NI-*Eco*RI 129-bp fragment of pBR322 plasmid (top strand); lanes 1–3, Maxam–Gilbert sequencing reactions of GA, CT, and G, respectively; lane 4, unmodified DNA treated with UVRABC (control); lane 5, DNA modified with 0.3 mM **1** after reductive activation with  $\text{Na}_2\text{S}_2\text{O}_4$  (0.6 equiv, three incremental additions); lane 6, DNA modified with 0.9 mM **1** after reductive activation with XO/NADH (XO = xanthine oxidase); lane 7, DNA modified with 0.45 mM **8** after reductive activation with  $\text{Na}_2\text{S}_2\text{O}_4$  (1 equiv, three incremental additions); lane 8, DNA modified with 0.45 mM **9** after reductive activation with  $\text{Na}_2\text{S}_2\text{O}_4$  (1 equiv, three incremental additions); lane 9, DNA modified with 0.9 mM **8** after reductive activation with XO/NADH; lane 10, DNA modified with 0.9 mM **9** after reductive activation with XO/NADH. The drug–DNA bonding-induced UVRABC nuclease incision bands (U1, U2, ..., U15) are labeled on the right side, and the numbers correspond to the guanine residues (1–15), which are numbered on the left side of the panel. Generally, UVRABC incises four nucleotides (occasionally three) 3' to modified G. The one-base ladders in lanes 5–10 are also observed in drug-modified DNA fragments without UVRABC (data not shown), and these bands likely resulted from depurination/depyrimidination during drug–DNA reaction. (B, right) Relative intensities (RI) of UVRABC nuclease incision of mitomycin **1**-, **8**-, and **9**-DNA adducts of a 69-base region within the 3'-end- $^{32}\text{P}$ -labeled *Bst*NI-*Eco*RI 129-bp sequence from the pBR322 plasmid. The concentration was 0.3 mM for **1** ( $\text{Na}_2\text{S}_2\text{O}_4$ ) and 0.45 mM for **8** and **9** ( $\text{Na}_2\text{S}_2\text{O}_4$ ). The intensities were normalized to 100% for the most intense band within each experiment. U1–U15 bands in lanes 5, 7, and 8 of (A) were scanned with a densitometer, and the relative intensity of each band was plotted at the corresponding G in the sequence.

the corresponding reaction done in the absence of DNA (HPLC analysis). Similarly, the temperatures selected for the **10**–DNA (37 °C) and **11**–DNA (22 °C) transformations were based on the observation that significant amounts of these mitosenes had undergone reaction in aqueous buffered solutions (pH 7.4) in the absence of DNA (HPLC analysis).

**B. Porfiromycins 8- and 9-DNA Bonding Profiles.** The autoradiogram and corresponding densitometric data for mitomycin C (**1**) and the C-10 halogen compounds **8** and **9** are provided in Figure 2. In these experiments we observed one-base ladders before (data not shown) and after UVRABC treatment (Figure 2A, lanes 5–10). These bands have been attributed to undetermined depurination/depyrimidination processes that occurred during the drug–DNA reaction. Accordingly, these bands were excluded in the drug–DNA bonding-induced UVRABC incision analysis. The intense band in the autoradiogram for the G(2) and G(3) region for the mitomycin C modification reaction (Figure 2A, lanes 5 and 6) has been

assigned to the G(2) site in the 5'CG(2)G(3)T locus rather than the G(3) position (Figure 2B). We have previously demonstrated that G(2) was extensively modified in this restriction fragment by determining the bonding profile for both the 3'- and 5'-end-labeled DNA (top strand). Moreover, we have reported that 5'CG\*G was the preferred sequence for mitomycin C monoalkylation transformations within a variety of DNA fragments, whereas drug bonding occurred with only low frequency at 5'GG\*T sites.<sup>6</sup> We observed that xanthine oxidase/NADH reductive activation (30 min) of the C-10 chloro adduct **8** and the C-10 bromo derivative **9** led to distinct DNA bonding sites on the basis of UVRABC incision analysis (Figure 2A, lanes 9 and 10). A similar finding was obtained when  $\text{Na}_2\text{S}_2\text{O}_4$  was used as the reductant (Figure 2A, lanes 7 and 8). The UVRABC digestion patterns for **8** and **9** (Figure 2A, lanes 7–10) were nearly identical and differed from **1** (Figure 2A, lanes 5 and 6). We observed that mitomycin C bonded preferentially at 5'CG\* sites, whereas **8** and **9** bonded at

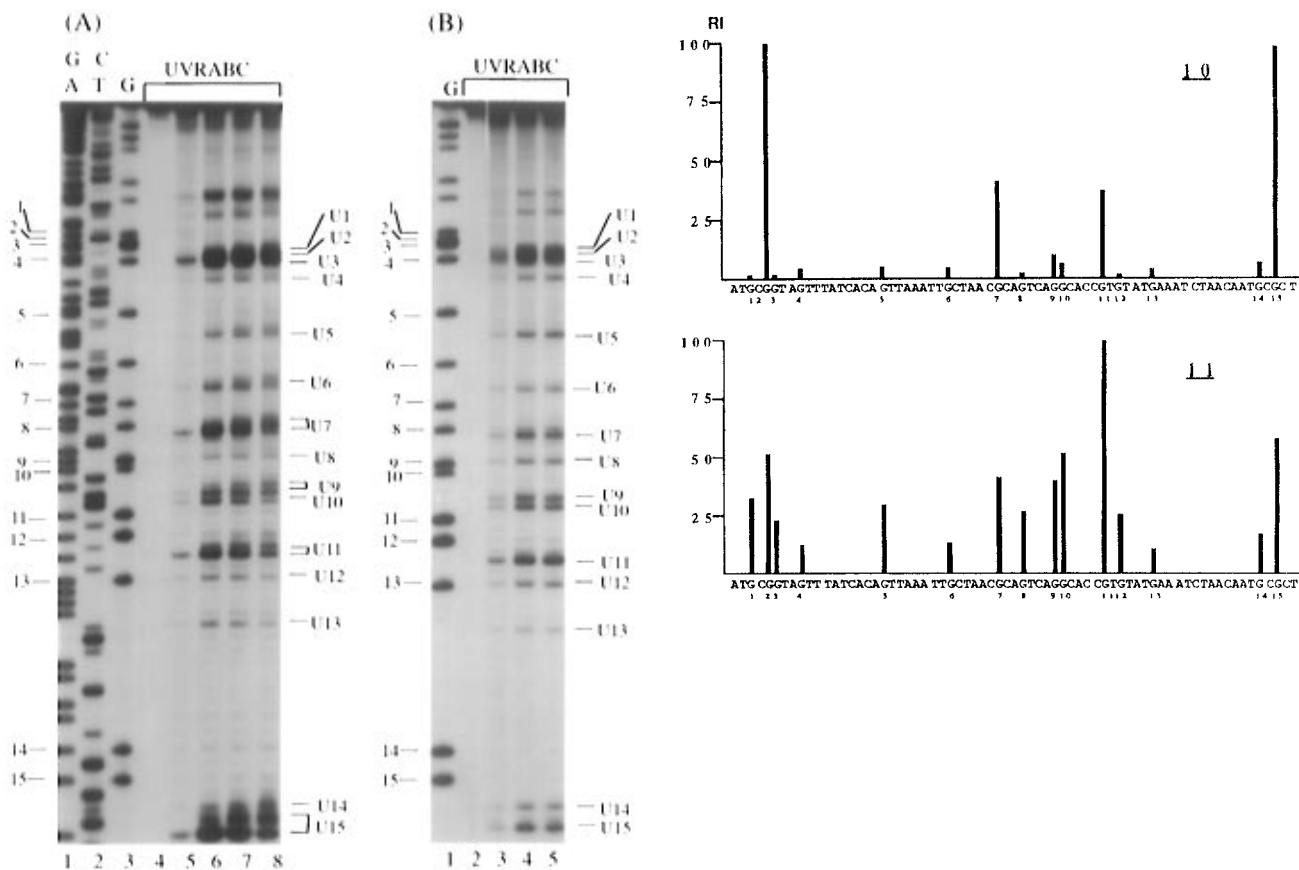


**Figure 3.** (A) Autoradiogram of UVRABC nuclease cutting of the mitomycin **10**-modified 3'-end- $^{32}\text{P}$ -labeled *Bst*NI-*Eco*RI 129-bp fragment from the pBR322 plasmid (top strand): lanes 1–3, Maxam–Gilbert sequencing reactions of GA, CT, and G, respectively; lane 4, unmodified DNA treated with UVRABC (control); lanes 5–8, DNA modified with 1.5 mM **10** after incubation at 22 °C (1 h), 37 °C (1 h), 37 °C (2 h), and 37 °C (3 h). The drug modification-induced UVRABC nuclease incision bands (U1–U15) are labeled on the right side of the panel, and the numbers corresponding to the guanine residues (1–15) are listed on the left. (B) Autoradiogram of UVRABC nuclease cutting of the mitomycin **11**-modified 3'-end- $^{32}\text{P}$ -labeled *Bst*NI-*Eco*RI 129-bp fragment from the pBR322 plasmid (top strand): lane 1, Maxam–Gilbert sequencing reactions of G; lane 2, unmodified DNA treated with UVRABC (control); lanes 3–5, DNA modified with 0.9 mM **11** after incubation at 22 °C for 5, 10, and 20 min, respectively. The drug modification-induced UVRABC nuclease incision bands (U1–U15) are labeled on the right side of the panel, and the numbers corresponding to the guanine residues (1–15) are listed on the left. (C, right) Relative intensities (RI) of UVRABC nuclease incision of mitomycines **10** (upper panel) and **11** (lower panel) adducts of a 69-base region within the 3'-end- $^{32}\text{P}$ -labeled *Bst*NI-*Eco*RI 129-bp sequence from the pBR322 plasmid. The concentration was 1.5 mM for **10** and 0.9 mM for **11**. The intensities were normalized to 100% for the most intense band with each experiment.

guanines but with considerably diminished selectivity (Figure 2B). Two different regions of the autoradiogram illustrated these changes. First, a significant decrease in the relative percent for G(2) bonding was observed for **8** and **9** over **1**. This nucleotide was one of three sites where appreciable mitomycin C (**1**) bonding occurred. Second, the site specificity demonstrated by **1** for 5'CG\*T (G(15)) over other guanine-containing trinucleotide sequences was noticeably diminished in the **8**- and **9**-DNA bonding processes. The diminished 5'CG\* sequence selectivity observed for reductively activated **8** and **9** transformations, as compared with **1**, was consistent with the proposed hydrogen bond interaction between the guanine 2-amino (G) proton in 5'CG\*5'CG sequences and the C-10 oxygen in the activated mitomycin.<sup>5,6,10</sup> Replacement of the C-10 oxygen substituent with either chlorine or bromine should diminish the strength of this hydrogen bond interaction.<sup>22</sup>

**C. Mitomycines 10- and 11-DNA Bonding Profiles.** It is possible that the diminished bond specificity of halides **8** and **9** could stem from a halogen effect rather than from a diminished hydrogen bond interaction between the guanine exocyclic 2-amino group on the nonbonding strand and the C-10 oxygen in the activated mitomycin. To determine this possibility, we

compared the DNA bonding profiles of *N*-methyl-7-methoxyaziridinomitomycin (**10**) with 7-methoxy-10-noraziridinomitomycin (**11**). Incubation of the 129-bp DNA with **10** (22 and 37 °C) led to exclusive guanine alkylation, with bonding occurring preferentially at the 5'CG\* loci (Figure 3A, lanes 5–8). Correspondingly, incubation of **11** with the DNA (22 °C) led to guanine modification with diminished sequence selectivity (Figure 3B, lanes 3–5). Comparison of the densitometric data for **10** and **11** revealed several noteworthy features (Figure 3C). For mitomycin **10**, the four most intense bonding sites corresponded to 5'CG\* sites. However, we observed that mitomycin **11** bonded most guanines and had only a slight preference for 5'CG\* sites. The only exception to this pattern was the 5'CG\* site at G(11), which was extensively modified. The diminished DNA bonding specificity observed for **11** was consistent with the notion that the C-10 oxygen substituent in the mitomycin facilitates preferential drug bonding at 5'CG\* sequences.<sup>5,6,10</sup>

**D. Kinetics of UVRABC Incision of Mitomycin-DNA Lesions.** The different intensities for the UVRABC incision bands at different sequences may reflect either different levels of drug modification or different efficiencies of UVRABC incision at different sequences. Although under our standard UVRABC reaction conditions (37 °C, 60 min) the level of

(22) Baker, E. N.; Hubbard, R. E. *Prog. Biophys. Mol. Biol.* **1984**, *44*, 97–179.

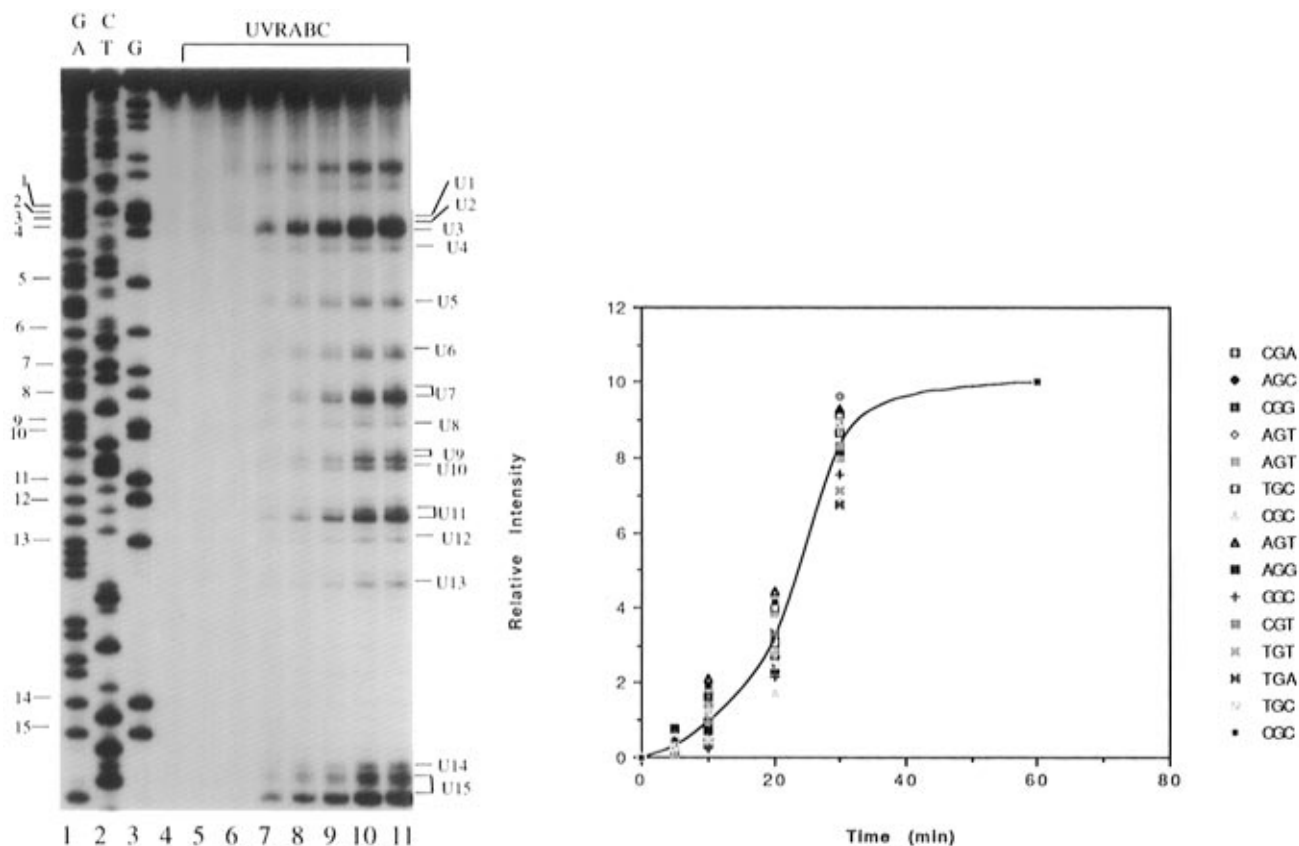


**Figure 4.** (A, left) Autoradiogram of UVRABC nuclease cutting of the *N*-methyl-7-methoxyaziridinomitosene (**10**)-modified 3'-end-<sup>32</sup>P-labeled *Bst*NI-*Eco*RI 129-bp fragment of pBR322 plasmid (top strand): lanes 1–3, Maxam–Gilbert sequencing reactions of GA, CT, and G, respectively; lane 4, native DNA without UVRABC cutting (control); lane 5, unmodified DNA treated with UVRABC (control); lane 6, DNA modified with 1.5 mM **10** was treated with UVRABC without incubation; lanes 7–11, DNA modified with 1.5 mM **10** was treated with UVRABC and incubated at 37 °C for 5, 10, 20, 30, and 60 min, respectively. (B, right) Time course of UVRABC incisions at different sequences on DNA fragments modified with 1.5 mM **10** (lanes 6–11). The different sequences are represented by different symbols. The line represents the mean value of the different sequences.

incision reached a plateau, we could not be certain that the drug–DNA adducts are completely incised by UVRABC. We, therefore, undertook incision kinetics analysis to distinguish these two possibilities.<sup>23</sup> Since there are no DNA polymerases and ligases present under our UVRABC reaction conditions, the result of UVRABC incision is irreversible.<sup>24</sup> Also, under our reaction conditions the enzyme/DNA molar ratio is greater than 1. We reasoned that if the efficiency of UVRABC incision on drug–DNA adducts is sequence dependent then the kinetics of incision would be different for various sequences. We chose *N*-methyl-7-methoxyaziridinomitosene (**10**)-modified DNA to examine the kinetics of the UVRABC incision process because mitosene bonding occurred efficiently and because the intensity of the drug-induced UVRABC incision band varied at different sites. Results in Figure 4A showed that the UVRABC incision at all the drug-bonding sites is a function of incubation time and appears to plateau after 30 min of incubation. Fifteen well-resolved bands were quantified, and the results in Figure 4B demonstrate that the kinetics of UVRABC incision at these sequences are virtually identical. On the basis of these results, we concluded that under our reaction conditions the degree of UVRABC incision represented the extent of drug–DNA bonding.

## Conclusions

In this study we sought to provide evidence that a hydrogen bond between the guanine 2-amino (G) protons in the non-

bonding strand of 5'CG\*•5'CG sequences and the C-10 oxygen in the activated mitomycin fosters mitomycin adduction to give **5** (Figure 1). We have tested this notion by determining the bonding profiles of **8** and **9** in which the C-10 oxygen substituent in the porfiromycin was replaced by a halogen moiety and by determining the bonding profile for 7-methoxy-10-noraziridinomitosene (**11**). In all three cases, diminished sequence selectivity for guanine adduction was observed at 5'CG\* sequences compared with suitable control substrates that contained a C-10 oxygen substituent. These findings are consistent with earlier studies<sup>5,6</sup> and recent NMR structural studies of the mitomycin C–DNA monoadduct<sup>25</sup> that have implicated this hydrogen bond in *in vitro* mitomycin C–DNA bonding transformations. The potential roles of other substituents within this compact, functionally rich antineoplastic agent are under investigation.

## Experimental Section

**Materials.** Mitomycin C (**1**) (pure) was supplied by Bristol-Myers Squibb Co. (Wallingford, CT). The C-10 halogen compounds **8**<sup>11</sup> and **9**<sup>11</sup> and mitosenes **10**<sup>12</sup> and **11**<sup>13</sup> were synthesized according to literature methods. Na<sub>2</sub>S<sub>2</sub>O<sub>4</sub> was purchased from Fisher Scientific Co. Restriction enzymes and DNA polymerase I (Klenow fragment) were obtained from New England BioLabs. NACS Prepacs convertible columns (NACS Pacs) were purchased from Bethesda Research Laboratories. Xanthine oxidase, NADH, and all other chemicals and electrophoretic materials were obtained from either Sigma Chemical Co. or Bio-Rad

(23) For a similar study, see: Chen, J. X.; Pao, A.; Zheng, Y.; Ye, X.; Kisleuoy, A.; Morris, R.; Slaga, T. J.; Harvey, R.; Tang, M.-s. *Cancer Res.*, submitted for publication.

(24) Van Houten, B. *Microbiol. Rev.* **1990**, *54*, 18–51.

(25) Sastry, M.; Fiala, R.; Lipman, R.; Tomasz, M.; Patel, D. J. *J. Mol. Biol.* **1995**, *247*, 338–359.

Laboratories. The [ $\alpha$ - $^{32}$ P]dTTP (specific activity approximately 3000 Ci/mmol) was purchased from DuPont-New England Nuclear.

**DNA Fragments Isolation and  $^{32}$ P End Labeling.** Plasmid pBR322 was purified by cesium chloride density centrifugation and dialyzed extensively against TE buffer (10 mM Tris·HCl, pH 8.0, 1 mM EDTA). The following procedure was utilized to isolate the 129-bp fragment, with  $^{32}$ P labeled at one of the 3' ends. The pBR322 plasmid was first digested with *Bst*NI, and the band corresponding to the 1857-bp fragment was isolated from a 1.4% agarose gel and cleaned by passing through a NACS Pac followed by ethanol precipitation. The 1857-bp fragment was labeled at the 3' terminus in the presence of [ $\alpha$ - $^{32}$ P]dTTP and Klenow fragment (5 units) in 10 mM Tris·HCl, pH 8.0, 5 mM MgCl<sub>2</sub>, and 7.5 mM DTT and incubated at 20 °C (30 min). The labeled DNA fragment was precipitated with ethanol and digested with *Eco*RI. The desired 129-bp fragment was purified by electrophoresis on a 5% polyacrylamide gel.

**Drug Bonding with Na<sub>2</sub>S<sub>2</sub>O<sub>4</sub>. DNA-Mitomycin (Porfiromycin) Monoalkylation Reactions.** Specified amounts of **1**, **8**, and **9** were added to the radioactively labeled DNA in 25 mM Tris·HCl buffer, pH 7.4, to give the desired final drug concentration. The solutions were deaerated with Ar (15 min), and then freshly prepared, deaerated, aqueous Na<sub>2</sub>S<sub>2</sub>O<sub>4</sub> solutions (total 0.6–1 equiv) were added in three incremental portions (20 min). The reactions were maintained at 22 °C (1 h) under Ar and then exposed to air.

**Drug Bonding with Xanthine Oxidase/NADH. DNA-Mitomycin (Porfiromycin) Monoalkylation Reactions.** Radioactively labeled DNA, drug (**1**, **8**, **9**), and NADH (2 equiv) were incubated in 100 mM Tris·HCl, pH 7.4, with xanthine oxidase (0.5 unit/ $\mu$ mol of drug) for 30 min at 37 °C under Ar and then exposed to air.

**DNA-Mitosene 10 Bonding.** Compound **10** was added to four tubes each containing the radioactively labeled DNA in 25 mM Tris·HCl buffer, pH 7.4, to a final concentration of 1.5 mM. The solution in tube 1 was incubated at 22 °C for 1 h. The solutions in tubes 2–4 were incubated at 37 °C for 1, 2, and 3 h, respectively. The unreacted drug was removed by phenol–chloroform extractions.

**DNA-Mitosene 11 Bonding.** Compound **11** was added to three tubes each containing the radioactively labeled DNA in 25 mM Tris·HCl buffer, pH 7.4, to a final concentration of 0.9 mM. The solutions in tubes 1–3 were incubated at 22 °C for 5, 10, and 20 min, respectively. The unreacted drug was removed by phenol–chloroform extractions.

**Kinetic Study of UVRABC Incision of Mitosene 10-DNA Adducts.** Radioactively labeled DNA fragments were modified with compound **10** (final concentration 1.5 mM) in 25 mM Tris·HCl, pH 7.4, at 37 °C for 1 h. The unreacted drug was removed by phenol–chloroform extractions. Six tubes with equal amounts of drug-modified DNA were prepared. Each tube was treated with the same amount of UVRABC nuclease and incubated at 37 °C for different time periods (0, 5, 10, 20, 30, and 60 min).

**Purification of UVRA, UVRB, and UVRC Proteins.** UVRA, UVRB, and UVRC proteins were isolated from *Escherichia coli* K12

strain CH296 (*recA*, *endA*/F'*lacI*<sup>Q</sup>) carrying plasmids pUNC45 (*uvrA*), pUNC211 (*uvrB*), and pDR3274 (*uvrC*).<sup>26</sup> The methods of purification were the same as described previously.<sup>27</sup> We termed the collective activity of UVRA, UVRB, and UVRC in recognition and incision of modified DNA as UVRABC nuclease.

**UVRABC Nuclease Reactions.** The UVRABC nuclease reactions were carried out in a reaction mixture (25  $\mu$ L) containing 50 mM Tris·HCl (pH 7.5), 0.1 mM EDTA, 10 mM MgCl<sub>2</sub>, 1 mM ATP, 100 mM KCl, 1 mM dithiothreitol, 15 nM UVRA, 15 nM UVRB, 15 nM UVRC, and substrate DNA. The mixtures were incubated at 37 °C (1 h), and the reactions were stopped by phenol–chloroform extractions followed by ethanol precipitation in the presence of aqueous NH<sub>4</sub>OAc (2.5 M). The precipitated DNA was recovered by centrifugation and washed with 80% ethanol.

**DNA Sequencing, DNA Sequencing Gel Electrophoresis, and Autoradiography.** The 3'-end- $^{32}$ P-labeled *Bst*NI–*Eco*RI 129-bp DNA fragment of pBR322 was sequenced by the method of Maxam and Gilbert.<sup>28</sup> The  $^{32}$ P-labeled fragments with or without various enzyme treatments were suspended in sequencing tracking dye (80% v/v deionized formamide, 10 mM NaOH, 1 mM EDTA, 0.1% xylene cyanol, and 0.1% bromphenol blue), heated at 90 °C (3 min), and quenched in an ice bath. The samples were applied to an 8% denaturing sequencing gel in parallel with the Maxam–Gilbert sequencing reactions. After electrophoresis, the gels were exposed to Kodak X-Omat AR film with an intensifying screen at –70 °C.

**Densitometric Scanning.** The intensities of UVRABC nuclease incision bands were determined with a Bio-Image Open Windows Version 3 System consisting of a Howtek Scanmaster 3+ and whole band analysis software.

**Acknowledgment.** We thank Ms. A. Pao and Mr. Y. Zheng for UVR protein purification, Ms. Y. Y. Tang for plasmid DNA purification, and Dr. A. Sancar (University of North Carolina–Chapel Hill) for providing *E. coli* strains containing UVR gene plasmids. We gratefully acknowledge Drs. A. M. Casazza and W. Rose and the Bristol-Myers Squibb Co. (Wallingford, CT) for the generous gift of mitomycin C, and Dr. M. Kasai and Kyowa Hakko Kogyo Co., Ltd., for providing us with mitomycin A. This study was supported by National Institutes of Health grants (CA29756, H.K.; ES03124, M.-s.T.) and a grant from the Robert A. Welch Foundation (E607, H.K.).

JA953871V

(26) Thomas, D. C.; Levy, M.; Sancar, A. *J. Biol. Chem.* **1985**, *260*, 9875–9883.

(27) Tang, M.-s.; Nazimiec, M. E.; Doisy, R. P.; Pierce, J. R.; Hurley, L. H.; Alderete, B. E. *J. Mol. Biol.* **1991**, *220*, 855–866.

(28) (a) Maxam, A. M.; Gilbert, W. *Methods Enzymol.* **1980**, *65*, 499–560. (b) Maxam, A. M.; Gilbert, W. *Proc. Natl. Acad. Sci. U.S.A.* **1977**, *74*, 560–564.